Kinetic Optimization of Bacteriorhodopsin Films for Holographic Interferometry

A. Seitz and N. Hampp*

Institute for Physical Chemistry, University of Marburg, Hans Meerwein-Strasse, Geb. H, D-35032 Marburg, Germany

Received: November 8, 1999; In Final Form: May 1, 2000

The M-lifetime of bacteriorhodopsin films for optical recording is a key parameter in obtaining a high light sensitivity, a high contrast ratio, and a high contrast decay time. An increase of the M-lifetime causes a proportional reduction of the light intensity required for optical applications. In bacteriorhodopsin variants such as BR-D96N, the M-lifetime can be tuned over several orders of magnitude by simply changing the pH value with respect to the proton availability in the matrix of the films. At low humidities, the proton transport steps linked to the photocycle limit the overall kinetics. A proton-diffusion-limited, two-state model (PDL2 model) for bacteriorhodopsin is introduced which allows us to model mathematically the optical excitation and thermal relaxation processes for both high and low humidities in bacteriorhodopsin films. Films containing wildtype bacteriorhodopsin and the variant D96N are compared in dependence on the pH value and the relative humidity at 20 °C. Of the investigated materials, only BR films containing BR-D96N can be used for recording at low light levels of 100 μW/cm^2. In a holographic interferometry experiment—a typical application where a high light sensitivity is a key issue—it is demonstrated to what high extent the water content in the films affects their suitability for recording at low light levels. Kinetically optimized bacteriorhodopsin films yield a more-than-30-fold improvement of sensitivity in holographic interferometry compared to dry bacteriorhodopsin films.

Introduction

Bacteriorhodopsin (BR) is found as two-dimensional crystals, the so-called purple membranes (PM), in *Halobacterium salinarum*. Because of its efficient photochemistry, its photoelectric and proton-pumping properties, and its excellent stability against chemical, thermal, and photochemical degradation, a technical utilization of BR was considered soon after its discovery. Quite a lot of proposals for possible applications have been published, many of them in the optical field (for review see refs 1−4). Photochromic BR films for transient optical recording utilize the outstanding photophysical properties of this biological photochrome, i.e., the high quantum yield of 64%[5,6] of its primary photoreaction; the lack of a refractory period after relaxation;[7] the large spectral shift of more than 150 nm; and, in particular, its excellent reversibility.

The parameters relevant for the application of the BR films depend in a complex manner on (1) the BR material used, i.e., the wildtype or one of the variants; (2) optional additives in the films; and (3) the fabrication procedure itself. BR films from different sources differ widely in their photo response.

For applications such as holographic interferometry, the light sensitivity is a key issue. In this paper the reasons for the varying light sensitivities and the photo response kinetics are discussed, and methods for optimizing the photo response for low-light-level applications are described and experimentally verified.

Photoconversion of BR at Reduced Humidity. The photochromism of BR and the light-driven proton translocation from the inner to the outer side of the halobacterial cell membrane are directly coupled. The chromophoric group in BR contains a retinylidene residue attached to the protein moiety via a Schiff base linkage to the amino acid lysine-216. After absorption of a photon, a cyclic sequence of molecular changes is observed which is called the photocycle (e.g., refs 8, 9) of BR (Figure 1).

The photochromism of BR is related to the isomerization of the retinylidene group as well as a reversible protonation change of the C=N double bond. Photoisomerizations and chromophore relaxation are fast processes compared to the deprotonation ($L \rightarrow M^I$) and the reprotonation ($M^{II} \rightarrow N$) steps, which determine the photokinetics of BR. In the vectorial proton transport through BR, a chain of amino acid residues is involved, in particular the aspartic acids 85 and 96 (D85, D96). In addition, quite a number of functional water molecules close to the retinal binding pocket of BR and in the proton exit channel play an important role in the proton transport pathway through BR.[10] Rather early it was detected that the water content affects the kinetics and the mechanism of the photoconversions.[11] Many papers have addressed this topic using different experimental techniques (e.g., refs 12, 13). From neutron diffraction data, a dependence of the $M^I \rightarrow M^{II}$ transition on the water content was derived.[14]

Characterization of BR Films. For optical applications it is desired to modify the photophysical properties of BR to meet the demands of the different applications more closely. A high light sensitivity, a high contrast ratio, and a high contrast decay time are needed for most applications.[1−4]

Five parameters characterize the photoresponse of a particular BR film. The first and most simple is the optical density OD of the BR film, which represents the number of light-sensitive molecules per area. The second parameter is the light sensitivity *S*, which describes the optical density change in dependence on the light energy exposed. Since this is quite a complex function, a suitable simplification is to use the initial light sensitivity S_{init}, which correponds to the sensitivity *S* at time *t*

* Author to whom correspondence should be addressed. E-mail: hampp@mailer.uni-marburg.de.

10.1021/jp993949k CCC: $19.00
Published on Web 07/07/2000

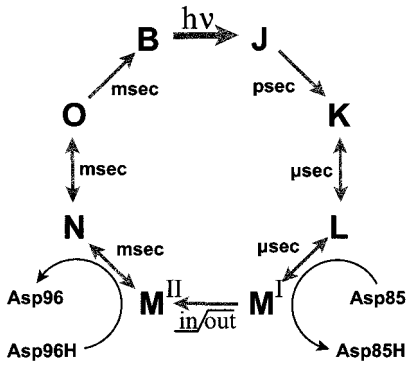

Figure 1. Schematic representation of the photocycle of bacteriorhodopsin. During L → M^I, the Schiff base linkage is deprotonated toward the outer proton half-channel. In the M^I → M^{II} step, the accessibility of the Schiff base nitrogen for protonation switches from the outer to the inner half-channel. Reprotonation of the Schiff base linkage occurs during the M^{II} → N transition from the inner side of the purple membranes.

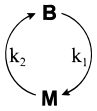

Figure 2. Simplified photocycle model for BR. This two-state model is often sufficient for the description of the photoconversions of BR.

= 0. The third parameter is the bleaching ratio R_B, which describes the intensity-dependent, steady-state absorption change of a BR film in relation to its initial optical density. The fourth parameter is the time τ_{50}, which is observed for the thermal decay of 50% of the initial contrast. Last but not least, the exposure E_{50}, required to obtain 50% of the maximal R_B-value, and the exposure S_{50}, required to bleach 50% of the initial optical density, are very useful values for the practical application of BR films.

Theoretical Section

Often a very simple two-state model (Figure 2) is good enough to approximate the photochemical conversions of BR.[15,16]

In the two-state model, k_1 represents the photochemical reaction rate from B to M, which is dependent on the actinic light intensity I and its wavelength λ, i.e., $k_1 = k_1(I, \lambda) := \alpha(\lambda) \cdot I$. Using $\epsilon_B(570\ \text{nm}) = 62\,700\ \text{l mol}^{-1}\ \text{cm}^{-1}$, $\Phi_{B\rightarrow M} = 0.64$, $\lambda = 570$ nm, the intensity I in mW/cm^2 and the Avogadro constant N_A, Planck's constant h, and the speed of light c for the conversion of the intensity into Einstein units, the result is

$$k_1 = \frac{2.303 \cdot \Phi_{B\rightarrow M} \cdot \epsilon_B(\lambda) \cdot \lambda \cdot I}{N_A \cdot h \cdot c} = \alpha(\lambda) \cdot I = 0.44 \cdot I[1/\text{s}] \quad (1)$$

and $\alpha_{570} = 0.44$ is obtained for the parameters given. For the wavelength 532 nm, $\alpha_{532} = 0.275$ is obtained for $\epsilon_B(532\ \text{nm}) = 42\,000\ \text{l mol}^{-1}\ \text{cm}^{-1}$.

The M-to-B reaction rate k_2 is indirectly proportional to the M-lifetime τ_M, i.e., $k_2 = 1/\tau_M$, as long as a simple first-order reaction is assumed. The temperature must be controlled in the experiments because τ_M is temperature-dependent. B_0 represents the total concentration of BR in the film. In the two-state model the relation $B_0 = B(t) + M(t)$ is valid at all times.

For the time dependence of bleaching the BR material, the following equation results:

$$B(t) = B_0 \cdot \frac{k_2 + k_1 \cdot \exp^{-(k_1+k_2)\cdot t_R}}{k_1 + k_2} \quad (2)$$

where t_R is the time after turning on the light. After the actinic light is turned off, the M-state returns thermally to the initial state. This is described by

$$M(t_D) = M_{SS}(I) \cdot \exp^{-k_2 \cdot t_D} \quad (3)$$

where t_D is the time after turning off the light. B_{SS} and M_{SS} represent the intensity-dependent, steady-state distributions of B and M.

$$B_{SS} = B_0 \cdot \frac{k_2}{k_1 + k_2};\ M_{SS} = B_0 \cdot \frac{k_1}{k_1 + k_2} \quad (4)$$

The time dependences of rise and decay of the B and M states in the two-state model are summarized in the following equations:

$$\begin{aligned} &\textit{rise} \\ B(t_R) &= B_{SS} + M_{SS} \cdot \exp^{-(k_1+k_2)\cdot t_R} \\ M(t_R) &= M_{SS} - M_{SS} \cdot \exp^{-(k_1+k_2)\cdot t_R} \\ &\textit{decay} \\ B(t_D) &= B_0 - M_{SS} \cdot \exp^{-k_2 \cdot t_D} \\ M(t_D) &= M_{SS} \cdot \exp^{-k_2 \cdot t_D} \end{aligned} \quad (5)$$

The intensity-dependent ratio between M and B in the steady-state γ results in

$$\gamma := \frac{M_{SS}}{B_{SS}} = \frac{k_1}{k_2} = \alpha \cdot I \cdot \tau_M \quad (6)$$

and depends on the wavelength-dependent factor $\alpha(\lambda)$, and—to the same extent—on the intensity I and the M-lifetime τ_M. This equation illustrates the importance of the M-lifetime for optical recording media. An increase in τ_M allows a proportional decrease in intensity to obtain the same γ value.

The bleaching ratio R_B, which describes the amount of BR material converted in the steady state from B to M in relation to the total amount of material present,

$$R_B := \frac{B_0 - B_{SS}}{B_0} = 1 - \frac{1}{1 + \alpha \cdot I \cdot \tau_M} = \frac{\gamma}{1 + \gamma} \quad (7)$$

depends on the γ-value. The R_B value ranges between 0% and 100%. For $\gamma > 1$, more than 50% bleaching is obtained.

The sensitivity of a BR film is initially at its highest value and then decreases constantly until the steady state is reached. The time dependence is complex. As a practically useful parameter, the exposure required to obtain 50% of the maximal bleaching of the BR material is introduced and named E_{50}. The time t_{50} to reach 50% of the final bleaching value, i.e., $B_{50} = 1/2(B_0 + B_{SS})$, is given in eq 8.

$$t_{50} = \frac{\tau_M \cdot \ln 2}{1 + \gamma} \quad (8)$$

In our experiments the intensity of the actinic light was not changed during the exposure. This means that the exposure required is obtained from

$$E_{50} := I \cdot t_{50} = \frac{I \cdot \tau_M \cdot \ln 2}{1 + \gamma} = \frac{\gamma}{1 + \gamma} \cdot \frac{\ln 2}{\alpha} = \frac{\ln 2}{\alpha} \cdot R_B \quad (9)$$

TABLE 1: Parameters for the Characterization of BR films for Optical Recording

	parameter	abbreviation	formula	key parameter
film preparation	optical density	B_0		
	M-lifetime	τ_M		
experiment	intensity	I		
	wavelength	λ		
application parameters	bleaching ratio	R_B	$= \gamma/(1+\gamma)$	$\tau_M \leftrightarrow I$
	rise time	t_{50}	$= \tau_M \cdot \ln 2/(1+\gamma)$	τ_M
	exposure required	E_{50}	$= R_B \cdot \ln 2/\alpha(\lambda)$	$\tau_M \leftrightarrow I$
	initial sensitivity	S_{init}	$= R_B \cdot t_{50} \cdot a(\lambda)/\ln 2$	τ_M
	contrast decay time	τ_{50}	$= \tau_M \ln 2$	τ_M

The initial sensitivity S_{init} describes the photoresponse of a BR film in the initial phase where the BR film behaves like a nonreversible material, e.g., a silver halide film. The S_{init} value of a BR film is defined as the intensity-dependent change of the population density of the B-state extrapolated to $t_R \rightarrow 0$.

$$S_{init} := \frac{dB}{dI}\Big|_{t\rightarrow 0} = \frac{\gamma}{1+\gamma}\cdot\frac{\alpha\cdot\tau_m}{1+\gamma} = \frac{\alpha}{\ln 2}\cdot R_B\cdot t_{50} \qquad (10)$$

The initial sensitivity S_{init} is dominated by the M-lifetime; the higher the value for τ_M, the higher S_{init} becomes. Particularly for applications where only low light levels are available, e.g., in interferometry, the M-lifetime is a key parameter.

Whereas the recording process needs quite a number of parameters for a proper characterization, the thermal relaxation to the initial state is characterized by one parameter only, i.e., the time τ_{50} for the thermal decay to 50% of M_{SS}. For the commonly used two-state model, the result is

$$\tau_{50} = \tau_M \cdot \ln 2 \qquad (11)$$

For our investigations, two definitions are introduced which take into account that the kinetics are often determined by difference spectroscopy. The first is M_{decay}, which describes the decay of the M-state population in relation to the initial M-state population M_{SS}. In analogy to this, $B_{recovery}$ is defined, which describes the return of the material to the B-state.

$$M_{decay} := \frac{\Delta M(t_D)}{\Delta M(max)} = \frac{M(t_D)}{M_{SS}(\gamma)}$$

$$\textit{and}\ B_{recovery} := \frac{\Delta B(t_D)}{\Delta B(max)} = -\frac{B(t_D) - B_0}{B_{SS}(\gamma) - B_0} \qquad (12)$$

In a two-state system, $B_{recovery}$ equals M_{decay} at all times. Plotting of $B_{recovery}$ against M_{decay} should reveal a straight line with a negative slope of 1. The time dependence of M_{decay} is the same as that of $B_{recovery}$.

$$\frac{dM_{decay}}{dt} = \frac{dB_{recovery}}{dt} = -k_2\cdot\exp^{-k_2\cdot t_D} \qquad (13)$$

Summarizing the above-introduced parameters shows that the M-lifetime indeed is a crucial point for optical recording media using BR and the key to low-light-level recording (see Table 1). However, care must be taken during film preparation so that the conventional two-state model is applicable for the ready-made BR films.

Experimental Section

Chemicals and BR-Material. PM used was prepared following the commonly used procedure.[17] Frozen PM was slightly sonicated in a water bath before use. All other chemicals were purchased from Sigma/Aldrich; these were of analytical grade and were used without further purification.

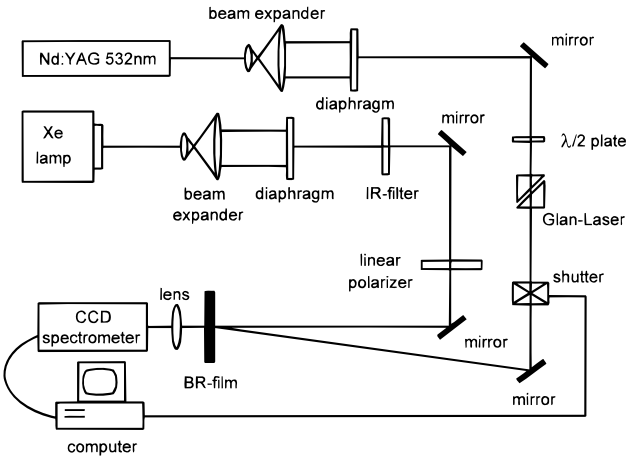

Figure 3. Experimental setup for the analysis of the intensity- and time-dependence of the B-state and M-state population in BR films.

Preparation of Bacteriorhodopsin Films. The samples were prepared by suspending PM in a 2.5% gelatine (Stoess AG) solution which was adjusted to the desired pH value by using a 2.5-mM arginine/asparagine/aspartic acid buffer of the desired pH value and filtering it through 5 μm nylon filters. All pH values mentioned in the paper refer to the pH value of the solution used to prepare the BR films. Because of the low water content of dried BR films, it is not feasible to give a pH value for them. The mixture was poured onto a glass substrate and then stored for 24 h at the desired relative humidity, which was adjusted by suitable salt solutions. Temperature and relative humidity were measured by a thermohygrometer (Ebro, TFH100). The optical density of the films used was in the range of OD-(570) = 0.6 to 1.1.

Difference Spectra. In Figure 3 the experimental setup for the analysis of the time dependence of the B-state and M-state population is shown schematically. A frequency-doubled Nd:YAG-laser (Coherent, DPSS 200) was used as actinic light source. The laser beam was expanded, and an inner part with nearly uniform intensity was separated by an iris diaphragm. The fine adjustment of the intensity was accomplished by a half-wave plate and a Glan-Laser prism. The intensity was measured with a calibrated powermeter (Newport, Model 835). Broad-band test light was obtained from a xenon lamp. After the beam was expanded, a small fraction was separated by a diaphragm and then passed through an IR filter to avoid undesired heating of the BR films investigated. By means of a linear polarizer, the polarization of the test light was adjusted to match the axis of the actinic light. After passing through the sample, the polychromatic test light was focused onto the entrance slit of a diode-array spectrometer (Oriel, Instaspec IV). A personal computer was used to control the diode-array spectrometer as well as the synchronization of the electromechanical shutter that controlled the actinic light. The white test light was 5 μW/cm^2 and weak enough that no detectable photoconversion levels were observed. All measurements were made at 20 °C. The BR films were adapted to light before analysis by flushing with white light from a xenon lamp (20 mW/cm^2) for 30 s.

Interferogram Analysis. The experimental setup used is shown schematically in Figure 4. The light reflected from the object is recorded by the BR film directly, i.e., lensless recording is used to obtain the maximal resolution. The reference wave incidents from the opposite direction compared to the object

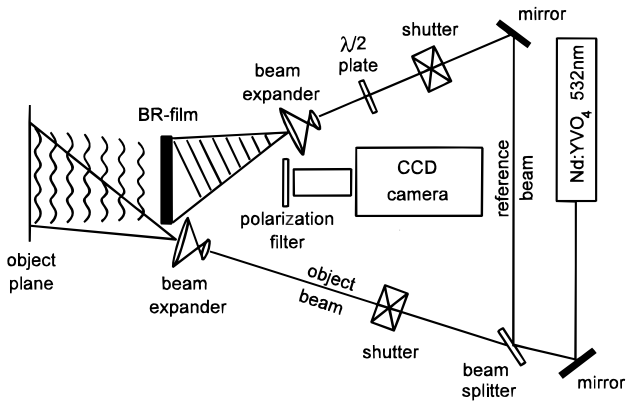

Figure 4. Experimental setup for reflection-type holographic recording.

wave and so-called reflection type holograms are formed. A more detailed description of the optical setup is found in ref 18. Interferograms were obtained in double-exposure technique. Three seconds elapsed between the first and second hologram recording. As test objects, ceramic motor valves were used. The exposure time per hologram was 0.3 s. For the illumination of the test objects, a frequency-doubled Nd:YVO_4 laser (Verdi Compass 2W, Coherent) operating at 532 nm was used. The effective intensity in the plane of the BR film was about 150 μW/cm^2.

Results

The simple two-state model (see Figure 2) is often employed to describe the photochemical behavior of BR. Contributions from early intermediates, i.e., K and L, may be neglected because of their short lifetimes (0.5 ps − 50 μs) as long as only absorption changes in the upper ms range are investigated (e.g., refs 19−22). In BR materials that have an extended M-lifetime, e.g., BR-D96N,[23] the population densities of the late intermediates N and O are also low. This is because the bottleneck in the photocycle are the M-states. For these reasons, BR materials with a substantially prolonged M-lifetime should in particular be sufficiently described by the above-mentioned two-state model.

Indicators that allow us to estimate whether the two-state model is sufficient for modeling a particular experiment are, first, that the decay of the M-state and the recovery of the B-state populations are directly correlated (see eq 12), and second, that in the difference spectra only absorption changes related to the B-state and the M-state are observed, i.e., that an isosbestic point is observed.

Relaxation after Photobleaching: M_{decay} versus $B_{recovery}$. The difference spectra for a BR-D96N film with pH = 10.5 and 30% RH after irradiation with actinic light of 2 mW/cm^2 for 260 s are shown in Figure 5. An isosbestic point at 452 nm is observed, which is in good agreement with ref 24. This observation proves that only two spectroscopically distinguishable intermediates contribute to the absorption changes. A well-defined isosbestic point was found for all humidities (20%−95% RH) for BR-WT and BR-D96N at pH values of 7.0 and 10.5.

To analyze the time dependence of the population density changes in B and M, it is not necessary to use the whole spectra. It is sufficient to plot the absorption changes at 570 nm, which represent the B-state population, and those at 410 nm, which characterize the M-intermediate population. For the determination of the concentrations, the applicability of the Beer−Lambert law is assumed.

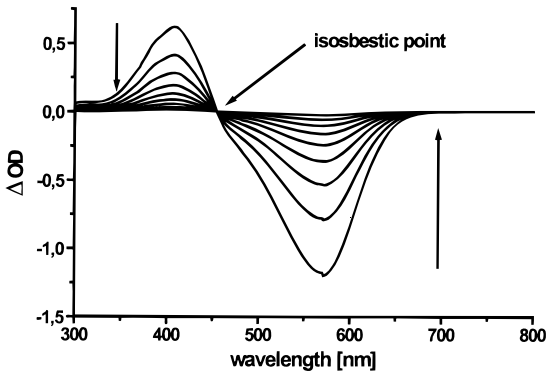

Figure 5. Difference spectra of the thermal decay to the initial state of a BR-D96N film after exposure. The BR film was bleached with an intensity of 2 mW/cm^2 at 532 nm for 260 s. During this time, the steady state was reached reliably. The different absorption spectra were subtracted from the absorption spectrum of the same BR film in its initial state. The arrows indicate the time evolution of the spectra which were recorded every 2 min. Only one isosbestic point at about 450 nm is observed. This indicates that only two spectroscopically distinguishable intermediates of BR contribute to this process.

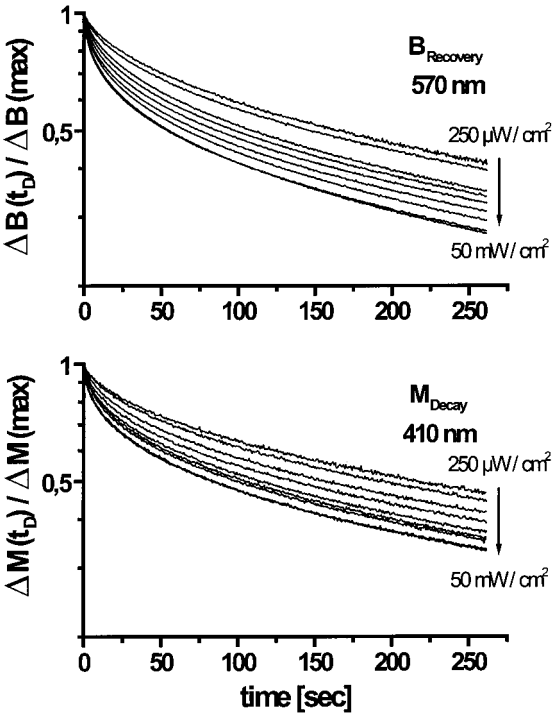

Figure 6. $B_{recovery}$ and M_{decay} for a BR-D96N film at low humidity. The film was equilibrated to 30% relative humiditiy. After light adaptation, the film was irradiated for 260 s with different intensities of actinic light (532 nm). The lowest intensity was 250 μW/cm^2 and corresponds to the uppermost relaxation curves. The arrows indicate increasing light intensities. From one curve to the next, the intensity was approximately doubled. The nine relaxation curves shown cover the wide intensity range for bleaching the BR film from 250 μW/cm^2 to more than 50 mW/cm^2.

In Figure 6 the $B_{recovery}$ and M_{decay} curves for a BR-D96N film at 30% relative humidity are shown representatively. They were measured after 260 s irradiation with different intensities of actinic light of 532 nm wavelength. Each line in the plots represents a different bleaching intensity in the range from 250 μW/cm^2 to about 50 mW/cm^2. From one curve to the next, the intensity was doubled. The curve corresponding to the lowest intensity used for bleaching the BR film is on the top. The arrows indicate the increase in light intensity. The *y*-axes are logarithmically scaled. In case the expected monoexponential

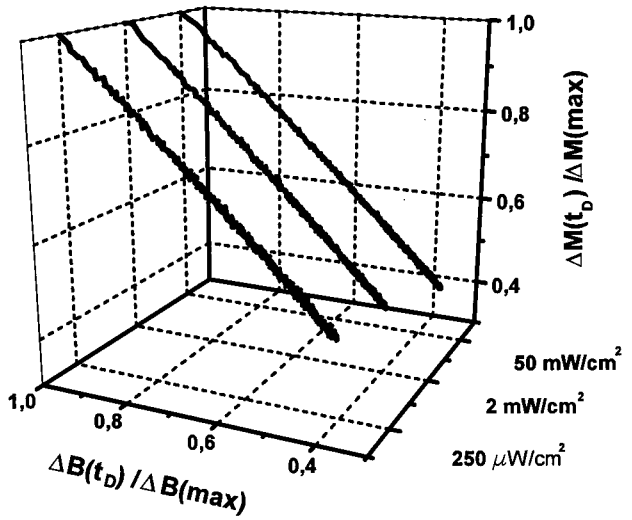

Figure 7. M_{decay} plotted depending on $B_{recovery}$ for three selected intensities. The same data as shown in Figure 6 were used. The linear relation between $B_{recovery}$ and M_{decay} proves that both states are affected to the same extent by the mechanism causing the deviations.

kinetics would be observed (see eq 13),

$$\frac{d}{dt}(\log M_{decay}) = \frac{d}{dt}(\log B_{recovery}) \approx -0.434 \cdot k_2 \quad (14)$$

straight lines should be obtained in Figure 6 with the same negative slope proportional to the M-lifetime. However, significant deviations from the expected monoexponential behavior are observed.

The next question is whether the deviations in $B_{recovery}$ and M_{decay} are the same. In Figure 7 $B_{recovery}$ is plotted against M_{decay} for three different intensities of actinic light. A straight line is obtained in all cases. This proves that the B-state and the M-state are affected to the same extent by the mechanism that causes the deviations, regardless of whether the photochemical rate is high or low.

Summarizing the experimental data so far leads to the conclusion that indeed, only the two spectroscopically distinct intermediates B and M are needed to describe the photoconversions (two-state model). The observed kinetic deviations must be caused by mechanisms that are related to the reversible deprotonation and reprotonation steps accompanying the photocycle.

M-Decay Kinetics at Reduced Humidity. In this section we investigate how the M-decay kinetics depends on the humidity and the material. For this purpose the BR films are bleached until the steady state is reached, and then the light is turned off and the M population returns thermally to the B-state. The decay behavior is analyzed for dependence on the actinic light level for various samples. It was found that at certain experimental conditions M_{decay} as well as $B_{recovery}$ are accelerated when the actinic light intensity is increased.

In Figure 8 the time τ_{50} is plotted against the R_B value $R_B = M_{SS}/B_0$ for BR-WT and BR-D96N films at different humidities. For BR films containing BR-WT or BR-D96N at high relative humidities, e.g., more than 90%, the τ_{50} time is independent of the R_B value. This result is expected for a first-order reaction, i.e., a monoexponential decay. Reducing the relative humidity changes the decay characteristics of the BR films and τ_{50} becomes dependent on the degree of bleaching, i.e., the R_B value. A linear dependency between the τ_{50} time and the R_B-value is observed for the BR-D96N film at 30% relative humidity (Figure 8A). The time τ_{50} is decreasing with increasing values for R_B.

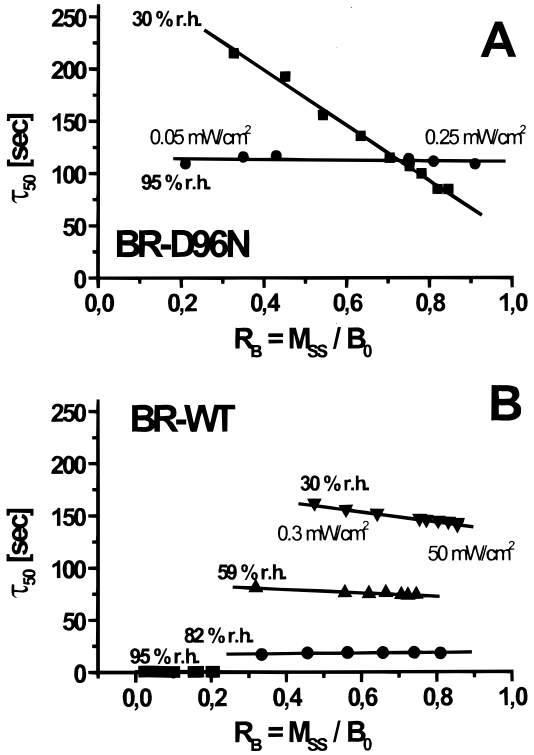

Figure 8. (A) Time τ_{50} for the M-decay plotted against the R_B value for a BR-D96N film at 30% and 95% relative humidity. A BR-D96N film with a pH value of 10.5 was exposed for 260 s to actinic light of 532 nm with various intensities. A linear dependence of τ_{50} on R_B is observed which indicates that the reaction from M to B follows a second-order reaction kinetics when the humidity in the film is low, e.g., 30%. In case of high water content, i.e., 95% relative humidity, no dependence on the initial bleaching value is observed (first-order reaction). (B) The same experiment, but for BR films containing BR-WT at pH 10.5. Two effects are observed. The first is that τ_{50} depends strongly on the humidity in the BR film. Higher τ_{50}values are obtained at lower humidities. The second is that at high humidities, the slope of the values is close to zero (no dependence on the R_B value) and increases with decreasing humidity.

This behavior is found to a different extent for both BR-WT (Figure 8B) and BR-D96N films, at low as well as at high pH values, as soon as the films are equilibrated to low relative humidities. In Figure 8B data obtained with BR films containing BR-WT at pH 10.5 are shown. Two effects are observed. The first is that τ_{50} depends strongly on the humidity in the BR films but to a lesser extent on the R_B value. Higher τ_{50} values are obtained at lower humidities. The second is that at high humidities, the slope of the values is close to zero (no dependence on the R_B value) and increases with decreasing humidity but to a lesser extent than observed for BR-D96N. In both plots, the intensities needed to obtain the lowest and the highest R_B value are given for one selected curve. Obviously, the BR-WT films (Figure 8B) require significantly higher intensities than the BR-D96N films (Figure 8A).

Mathematical Analysis of the Decay Kinetics. Analyzing the M-decay characteristics reveals striking deviations from a first-order reaction. For BR-D96N at pH 10.5 and 95% RH (Figure 9A), a perfect first-order reaction is obtained. In the representation chosen, where the *y*-axis is logarithmically scaled, a straight line is expected for a first-order reaction. The residual plot proves that no contribution other than the monoexponential one corresponding to a $\tau_{50} \approx 125$ s occurs.

For BR-D96N at pH 10.5 and 30% RH (Figure 9B), a second-order temporal decay characteristic is obtained which appears

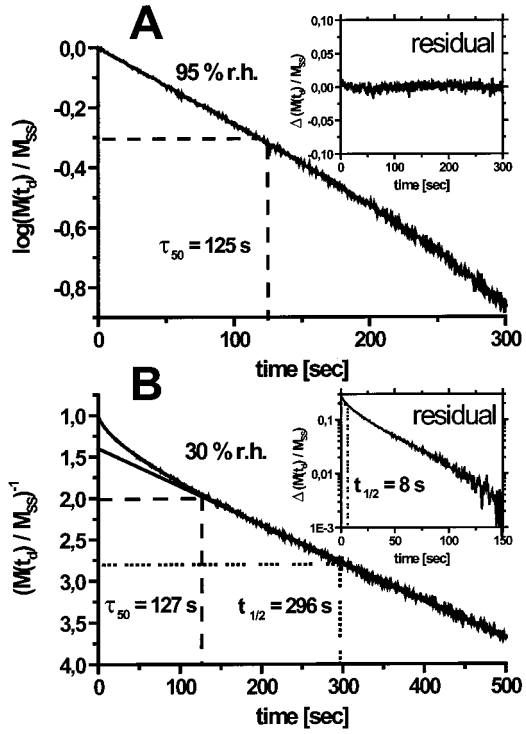

Figure 9. Temporal characteristics of the thermal decay of M in a BR-D96N film pH 10.5 in dependence on the relative humidity. (A) For high humidities (95%), the decay of the M state is monoexponential. A straight line in the logarithmic plot and the residual function close to zero support this assignment. (B) For low humidities (30%), the M decay is composed of a fast exponential (see residual with logarithmic *y*-axis) and a slow component which follows a second-order kinetics.

as a linear decay curve when a reciprocally scaled *y*-axis is chosen. In the very first part of the decay curve, which has about the same $\tau_{50} \approx 127$ s as the film at 95% RH (Figure 9A), an exponential contribution is observed (see residual plot). Whereas the exponential component has a rather short time constant of $t_{1/2} \approx 8$ s the second-order reaction component has a time constant more than 30-fold higher, $t_{1/2} \approx 296$ s.

Several groups have reported that the M-decay does not follow a first-order kinetics under certain conditions. Often a multiexponential fit is used. Parallel photocycles[25,26] were suggested as were cooperative effects[27−29] of BR molecules in the BR trimers that were found. Based on the experimental observation that in dependence on the humidity, a second-order reaction describes the M-decay well, and the fact that no other spectroscopically distinguishable states except B and M occur, we suggest a modified version of the simple two-state model which is in particular useful for the characterization and optimization of BR films.

Humidity-Dependent Alteration in the Photocycle Model. A modified two-state model of the BR photocycle is shown in Figure 10 which covers both high and low humidity. The model on the left is identical to the two-state model shown in Figure 2. When water is removed from BR it is replaced by the proton-diffusion-limited, two-state model (PDL2 model) in the middle. The black-colored parts represent the rate-determining pathways. The intermediates and pathways given in gray do not determine the kinetics but are needed for the following discussion.

At high proton availability (Figure 10, left), the photocycle is kinetically determined by $k_1(I)$ and $k_2(\tau_M)$. The deprotonation of the Schiff base to D85 and the reprotonation from D96N decouple the photochemical conversions from the proton-diffusion steps in the cytoplasmatic and extracellular half-channels.[12,30−32] In the variant D96N, the reprotonation of the Schiff base (broken line) occurs directly from the cytoplasmatic side of the membrane and therefore becomes dependent on the external proton availability.

At low humidity (Figure 10, middle), the $M^I \rightarrow M^{II}$ transition is hindered and BR is trapped in the M^I state.[14] The thermal decay rate k_6 from M^I to B is the transition for which we found a reaction kinetics that is mathematically described as a second-order reaction. The question arises which molecular mechanism could be responsible for a second-order kinetics of the M-decay at low humidities. The conformational reorientation of the Schiff base nitrogen in the $M^I \rightarrow M^{II}$ transition from the extracellular to the cytoplasmatic half-channel cannot take place,[14] and the Schiff base nitrogen in M^I is accessible only from the cytoplasmatic side, where D85H is positioned. Before M^I decays thermally, a stoichiometric reprotonation is required. The release of a proton from the terminal extracellular proton release group,[33] i.e., the dyad E194/E204, to the outer side of the membrane is triggered by the $L \rightarrow M^I$ transition.[34,35]

As long as the available number of protons H^+ is orders of magnitude higher than the number of BR molecules, the uptake of a proton through the extracellular half-channel is a pseudo-first-order reaction dependent on the M^I concentration only. If the proton availability reaches a level where the stoichiometric changes become relevant, a second-order reaction for the recombination of a proton with the proton acceptor in the dyad is expected. The related rate constant k_5—which determines the overall kinetics of the M^I decay—shows a second-order reaction kinetics.

$$H^+ + \mathrm{dya} \xrightarrow{k_5} \mathrm{dyaH} \bowtie \mathrm{D85H} + M^I \overset{k_4}{\rightleftharpoons} L \xrightarrow{k_6} B \qquad (15)$$

The protonation of the dyads E194/E204 and D85 are intimately linked. This connection is symbolized by the $\bowtie$ in eq 15. For this reason, the M^I decay appears to be stoichiometrically linked to the proton availability. The number of deprotonated dyads (dya) is equivalent to the BR molecules trapped in the M^I state.

$$\frac{dM^I}{dt} = -k_5 \cdot [H^+][\mathrm{dya}] = -k_5 \cdot [M^I]^2 \qquad (16)$$

From eq 16 values of $\tilde{M}(t_D)$ and $\tilde{\tau}_{50}$ are derived which correspond to the $M(t_D)$ and τ_{50} of the two-state model.

$$\tilde{M}(t_D) = \frac{M_{SS}}{1 + k_4 \cdot M_{SS} \cdot t_D} \; \textit{and} \; \tilde{\tau}_{50} = \frac{1}{k_4 \cdot M_{SS}} \qquad (17)$$

To determine whether the M-decay in a BR film follows a second-order reaction, the values for $\tilde{\tau}_{50}$ are plotted against R_B and M_{SS}, respectively (see Figure 8A,B).

In the experiment, a mixture of BR materials that may be described by the conventional two-state model and the PDL2-model is observed in dependence on the humidity level. This observation explains the complicated kinetic behavior found in the transition regime.

Contrast Decay Time τ_{50}. The above-described finding has quite an impact on the applications of BR films in optical recording. High M_{SS} values speed the decay of M and the related contrast between exposed and unexposed areas in BR films, but these two values should be independent.

In addition, this mechanism makes it almost impossible to compare samples from different labs. As shown in Figure 8, the τ_{50} time of the $M \rightarrow B$ reaction varies between 220 and 80 s in the same BR film, depending on the amount of M generated before turning off the actinic light. In addition, τ_{50} depends on

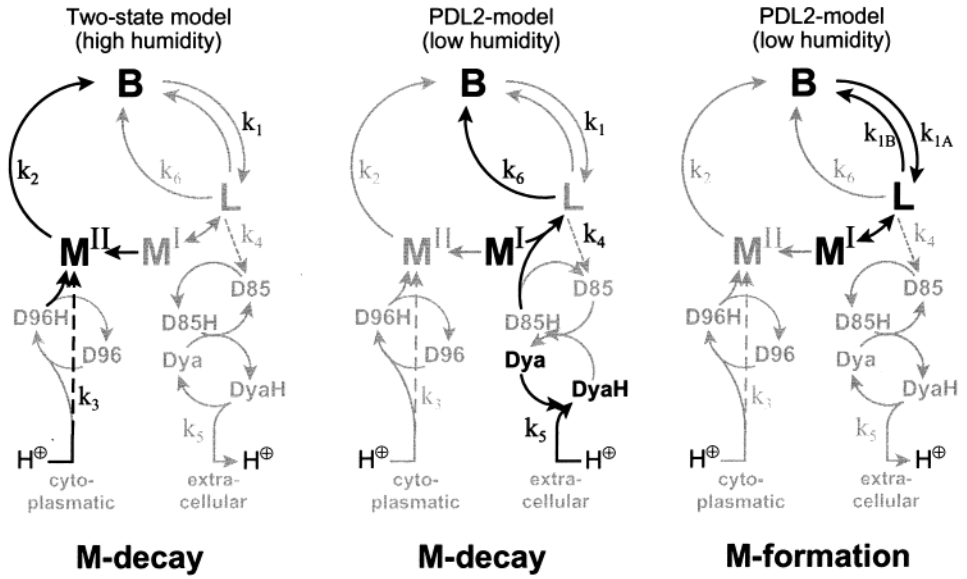

Figure 10. Two-state models for the BR photocycle at high and low humidities. Depending on the humidity, different pathways in BR determine the kinetic behavior. The black-colored parts represent the rate-determing pathways. (Left) At high humidities, the conventional two-state model is applicable to describe the M-decay. (Middle) At low humidities, the proton-diffusion-limited, two-state model (PDL 2 model) describes the M-decay which appears as a second-order reaction. The rate-determining step is the uptake of a proton from the outside of the membrane to the proton release complex (dyad = E194/E204). (Right) The kinetics of the M-formation is decreased in all cases where a population of the photoactive L-state occurs. Photochemical conversion of the L-state back to the B-state reduces the apparent light sensitivity of the BR film.

the temperature and the relative humidity. Measuring the decay of the M population in such films is not suitable for determining their M-lifetimes because the rate-determining process is the proton transition.

M-Formation at Reduced Humidity. In the experimental conditions where an accumulation of M^I occurs, a decrease of the light sensitivity is observed. An equilibration between M^I and L at reduced humidities is described in the literature.[36−38] The L concentration in dried samples was found to be low.[32] An increase in the L population reduces the net forward reaction rate $k_{1A} - k_{1B}$ (see Figure 10) because L is photochemically converted back to B. A BR film for which this process has to be considered appears less sensitive to light than a BR film for which the conventional two-state model may be applied.

As soon as M^I gets trapped, a population of the L-state proportional to the M^I population is assumed, i.e., $L: = \delta \cdot M^I$ with $\delta \ll 1$. The population of M^I in this model results from $B_0 = B + L + M^I$ to

$$M^I = \frac{B_0 - B}{1 + \delta} \tag{18}$$

The depopulation rate of the B-state, which is related to the sensitivity of the BR film, is given by

$$\frac{dB}{dt} = -k_1 \cdot B + k_1 \cdot (B_0 - B) \cdot \frac{\delta}{1 + \delta} \tag{19}$$

When such a BR film is bleached initially ($B \approx B_0$), the same response $dB/dt = -k_1 \cdot B$ is observed as for the idealized case. The more the BR film is bleached and B is depopulated, the more the second term in eq 19 becomes important and the speed of the depopulation of B decreases.

Experimentally, the effective forward rate k^*_1 can be determined by

$$k^*_1 = \frac{(1 - T) \cdot \Phi}{B + L} \cdot \frac{\lambda}{h \cdot c \cdot N_A} \cdot I \tag{20}$$

where T is the transmittance of the sample at 532 nm and $(1 - T)$ is the amount of light absorbed inside the sample, Φ is the quantum yield of the reaction, and $B + L$ is the concentration of BR in the B- and L-states. I is the light intensity in W/cm^2, λ is the wavelength, h is Planck's constant, c is the speed of light, and N_A is the Avogadro constant.

Measuring the transmitted light intensity and comparing the absorbed photons to the number of BR molecules allows us to measure how many photons statistically are needed per one B → M transition.

The rate of the M formation, i.e., M^I formation, may be expressed in the PDL2 model in terms of the B concentration similar to the two-state model.

$$\frac{dM}{dt} = k^*_1(I) \cdot B - k_5 \cdot M^2 \tag{21}$$

Please note that eq 21 is identical to eq 16 for $I = 0$.

In the following, we test whether the PDL2 model is suitable for the description of the kinetic behavior of BR in dry films.

Light Sensitivity of BR Films. The depopulation of the B-state depending on the exposure, i.e., intensity and time, is a very important factor in the characterization of BR films. We investigated the bleaching reactions of BR-WT and BR-D96N films depending on the relative humidity and at different pH values.

Representatively, the results obtained for a BR-D96N film at pH 7 will be discussed in detail. The results for BR-WT films at pH 7 and BR-WT as well as BR-D96N films at pH 10.5 can be interpreted in the same way.

In Figure 11 the depopulation of the B-state for a BR-D96N film at pH 7 and 30% respectively 95% relative humidity is shown. The intensity of the 532-nm actinic light was varied between 220 μW/cm^2 and about 20 mW/cm^2. The exact values are given to the right of each curve. The solid lines represent the experimentally obtained values, whereas the broken lines are the best fits to the measured values according to the simple two-state model of BR (see eq 4).

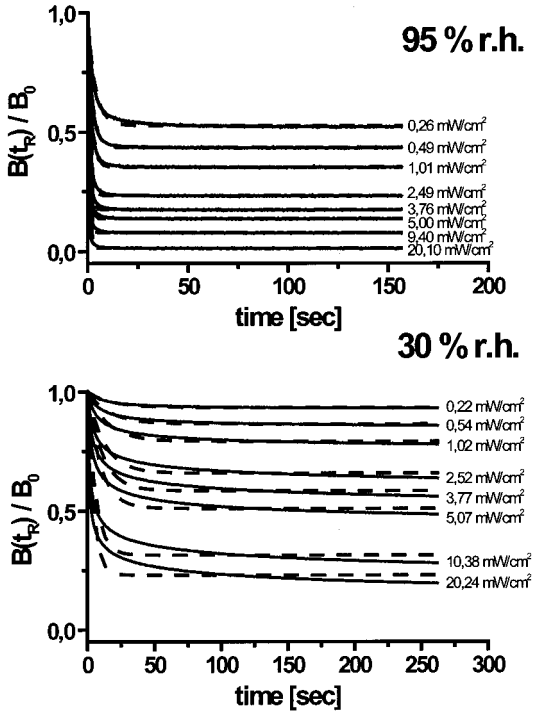

Figure 11. Depopulation of the B-state in a BR-D96N film at pH 7 at two different relative humidities, i.e., 95% and 30%, at different intensities of 532-nm actinic light. The intensity was varied between 220 μW/cm^2 and 20 mW/cm^2. The exact intensities are given to the right of each curve. Solid lines represent the experimental data, whereas the broken lines represent the best fit based on the conventional two-state model of BR. Whereas for the film at 95% humidity the two-state model describes the B depopulation properly, for the 30% film significant deviations are observed.

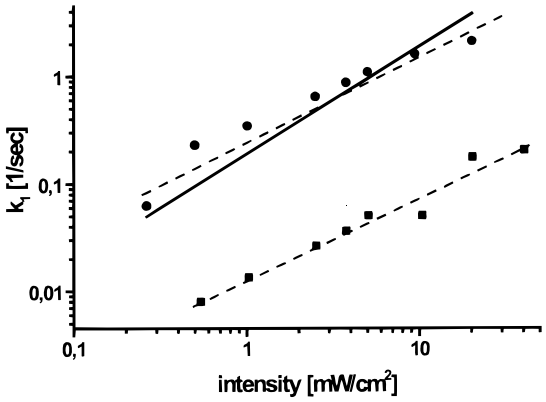

Figure 12. Values for the apparent photochemically induced reaction rate k_1 obtained from the numerical fit of the experimental data (see Figure 10). The values for k_1 for 95% relative humidity (●) are in good agreement with the theoretically predicted k_1 values from the two-state model (solid line). The k_3 values for 30% relative humidity (■) also show a linear dependency on the intensity, but they are about 1 order of magnitude worse than those at 95%.

In Figure 12 the calculated values for k_1 are plotted against the intensity of the actinic light. The theoretical values (two-state model) are represented by the solid line. In the diagram both axes are plotted on a logarithmic scale. For the theoretical values and the measured values, we found the expected linear dependency between the reaction constants k_1 and the intensity of the actinic light. The values obtained from the numerical fits (circles = 95%, squares = 30%) demonstrate that the film at 95% RH may be sufficiently described by the two-state model. The same BR film brought to 30% RH has a light sensitivity of about 1 order of magnitude lower.

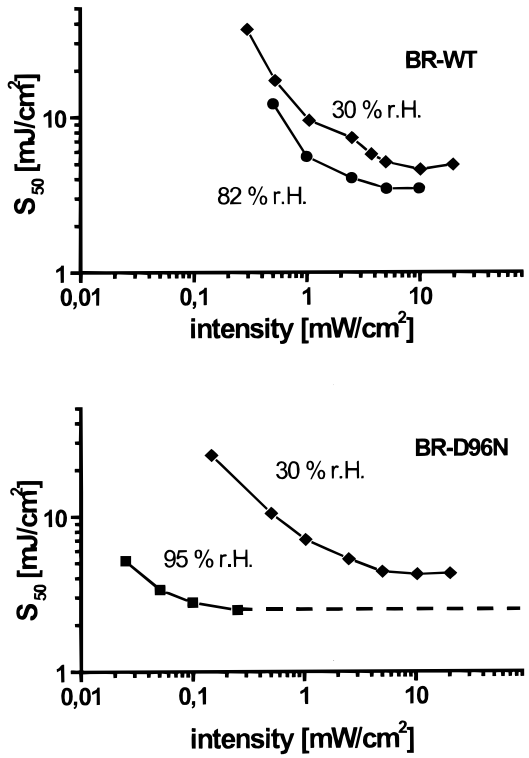

Figure 13. Energy required to bleach 50% of the BR material in films depending on the relative humidity. Both films shown, i.e., a BR-D96N film and a BR-WT film, had a high pH value of pH = 10.5. With decreasing relative humidity, i.e., decreasing amount of water in the film, the exposure required increases. The reason for this behavior is the hindered reaction from B to M. With the BR-WT film at 95% relative humidity, 50% bleaching could not be obtained.

To determine the sensitivity of BR films, we introduced E_{50}, the exposure required to bleach at a level of 50% of the maximal R_B value. A model-independent parameter, which is important in particular for applications in holography, is the energy S_{50} required to bleach 50% of the initial optical density B_0. For this value it is not necessary to determine the M-lifetime and the R_B value, which causes some problems in particular for films with short M-lifetimes.

In Figure 13 the energy for 50% bleaching (S_{50}) is plotted against the intensity of the actinic light for BR-D96N and BR-WT films at pH 10.5 for different relative humidities. With decreasing relative humidity, the sensitivity of the material is decreased. For the BR-WT film at a relative humidity of 95% with the light intensities in the experiment, 50% bleaching could not be obtained.

In Table 2 the characteristic parameters of BR-WT and BR-D96N films are compared with the values obtained from the two-state model simulation.

For BR-D96N at high relative humidities, an almost perfect match with the two-state model is obtained. Lowering the relative humidity causes a steady transition into the regime where the second-order kinetics is dominating the thermal relaxation of the M-state. This behavior is a reliable indicator that the properties for optical recording are not optimal.

The BR-WT films show a different behavior. Decreasing the humidity causes a steady increase in the apparent M-lifetime. At 30% RH about the same value is reached as in D96N. Whereas E_{50} is in the same range as for BR-D96N, the R_B values are significantly lower. The performance of BR-WT shows an optimum at slightly reduced humidity in the range of 70−80% RH This is difficult to adjust during film preparation to be long-lasting.

TABLE 2: Parameters Characterizing BR films at Different Relative Humidities

BR-D96N, pH 10.5, 20 °C, $I = 1$ mW/cm^2, $\lambda = 532$ nm										
					R_B [%]		E_{50} [mJ/cm^2]		S_{50} [mJ/cm^2]	
relative humidity	M-decay curve form	τ_{50} [s]	τ_M [s]	γ	theor	experim	theor	experim	1 mW/cm^2	100 μW/cm^2
95%	mono exp	136.0	196.2	53.86	98%	98%	2.45	2.78	2.46	2.79
82%	mono exp	133.0	191.9	52.67	98%	89%	2.46	3.08	2.99	4.87
72%	(transition)	129.8	187.3	51.40	98%	88%	2.46	3.48	3.54	5.55
59%	2nd order	142.1	205.0	56.27	98%	86%	2.47	4.05	4.03	7.67
30%	2nd order	150.2	216.7	59.48	98%	66%	2.47	6.76	6.95	33.62
BR-WT, pH 10.5, 20 °C, $I = 1$ mW/cm^2, $\lambda = 532$ nm										
					R_B [%]		E_{50} [mJ/cm^2]		S_{50} [mJ/cm^2]	
relative humidity	M-decay curve form	τ_{50} [s]	τ_M [s]	γ	theor	experim	theor	experim	1 mW/cm^2	100 μW/cm^2
95%	mono exp	0.3	0.4	0.13	12%	5%	0.50	2.68	*a*	*a*
82%	mono exp	18.7	27.0	7.41	88%	69%	2.21	2.41	5.64	*a*
72%	(transition)	41.7	60.2	16.47	94%	84%	2.37	3.01	3.98	*a*
59%	(transition)	75.4	108.8	29.86	97%	81%	2.43	4.16	5.19	*a*
30%	2nd order	147.4	212.7	58.37	98%	78%	2.47	5.16	9.85	*a*

[a] 50% bleaching was not reached; for this reason no experimental values are available.

Looking at the required exposures S_{50}, when intensities of 1 mW/cm^2 and 0,1 mW/cm^2 are employed, shows that the total sensitivity for medium light sensitivities (1 mW/cm^2) for BR-WT and BR-D96N films is of the same order of magnitude. But at low light levels, i.e., 100 μW/cm^2, only the BR-D96N films allow recording. For low light levels, the difference between films with low and high humidity is striking.

Performance of Kinetically Optimized BR Films for Low-Light-Level Recording in Holographic Interferometry. In holographic interferometry only low light levels are available. In this application, the sensitivity of the BR films is a key parameter. Whereas it is easy to determine that the BR-D96N films have significant advantages over BR-WT films in this application, the manufacturing procedure of the BR film is a key technology.

In the following example, the difference between a suitably prepared and an unsuitably prepared BR-D96N film is presented. Two BR-D96N films with water contents corresponding to the relative humidities 30% and 90% are compared. The experimental setup and the principles of holographic interferometric applications are described elsewhere.[18] The results obtained are shown in Figure 14. After an initial load of 500 N, an additional force of 40 N was applied to the shaft of the ceramic valve. In the upper part of the diagram, the recorded interferogram is shown. In the lower part, line-scans through the recorded interference patterns are given. The exposure time of the CCD camera was reduced by a factor of 3 in the case of the film with 90% relative humidity compared to the value of the 30% RH film. The contrast ratio of the interferogram is improved at least 10-fold when the 90% RH film is used instead of the 30% RH film. Taking further into account the 3-fold reduced shutter time for the 90% RH film, a 30-fold-increased sensitivity is obtained.

This example shows that it is essential to analyze the BR films used in an application carefully. The parameters introduced allow us to characterize a BR film reliably and to derive the parameters that are relevant for the optical applications.

The light sensitivity of such kinetically optimized BR-D96N films is about 30-fold higher than that of less carefully prepared films. BR-WT films cannot cover this intensity regime, which is typical in holographic interferometry.

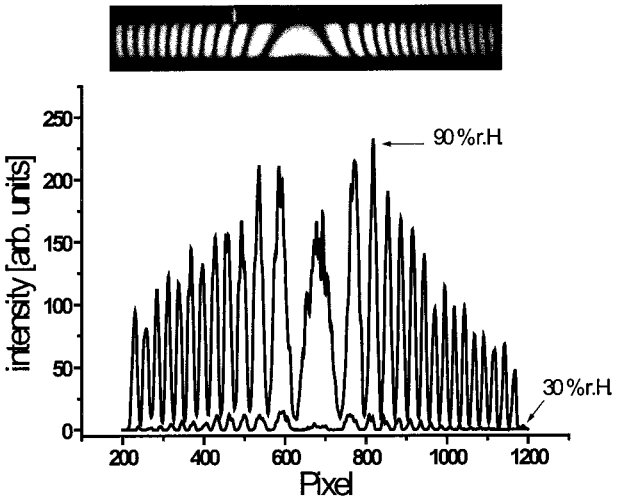

Figure 14. Line plots through an interferogram of a bended ceramic valve shaft recorded in double-exposure technique. Two BR films (BR-D96N, pH 10.5) with water contents corresponding to two different relative humidities (30% and 90%) were used. The exposure time was 0.3 s at an effective intensity of 0,15 mW/cm^2 in both cases. In the upper part appears the recorded interferogram. The shutter time of the CCD camera was one-third for the 90% film compared to the 30% film. The BR film with the higher water content shows a 30-fold-improved sensitivity compared to the BR film with the lower water content.

Conclusions

The properties of optical films made from BR-WT and BR-D96N change significantly depending on the amount of water in the films. At low and high water contents as well as low and high pH values, only the B-state and the M-state have to be considered for modeling the absorptive changes occurring during recording and erasure. With decreasing water content, the kinetic behavior changes. The light sensitivity of BR films decreases due to the photochemical back-reaction of L intermediate. L is populated through the equilibrium with M^I as soon as M^I gets trapped at low humidities.

The thermal decay of M is well-described at high humidities by the conventional two-state model, but at low humidities the PDL2 model is more appropriate for modeling the experimental data. The second-order reaction characteristics of the M-decay in dried films is linked to the reprotonation characteristics of the terminal proton release dyad E194/E204.

Optimization of BR films for low light intensities requires that the films be manufactured in such a way that the two-state model can be applied, i.e., not by hindrance of the $M^I \rightarrow M^{II}$ transition. Estimating whether a BR film meets these demands

can be done easily by determining the kinetics of the M-decay. Changes in the M-formation are accompanied by changes in the M-decay.

For films that follow it the two-state model shows that the M-lifetime is the key to the overall optimization of the kinetic behavior of such films because all technically relevant parameters, i.e., R_B, E_{50}, t_{50}, S_{init}, and τ_{50} depend on the M-lifetime. The figure of merit for the further improvement of BR films is to achieve further extended M-lifetimes in compositions that are accurately described by the two-state model.

Acknowledgment. This work was supported by the Federal Ministry for Education and Research (BMBF) through grant FKZ 01M2988A. We thank Volker Schwass for preparing the BR materials. Intensive discussion and help in the molecular interpretation of the experimental results by Dieter Oesterhelt is gratefully acknowledged.

References and Notes

(1) Oesterhelt, D.; Bräuchle, C.; Hampp, N. *Q. Rev. Biophys.* **1991**, *24*, 425.
(2) Vsevolodov, N. N. *Biomolecular Electronic. An Introduction via Photosensitive Proteins*; Birkhauser: Boston, 1998.
(3) Birge, R. R. *Annu. Rev. Phys. Chem.* **1990**, *41*, 683−733.
(4) Birge, R. R.; Gillespie, N. B.; Izaguirre, E. W.; Kusnetzow, A.; Lawrence, A. F.; Singh, D.; Song, Q. W.; Schmidt, E.; Stuart, J. A.; Seetharaman, S.; Wise, K. J. *J. Phys. Chem. B.* **1999**, *103*, 10746−10766.
(5) Govindjee, R.; Balashov, S. P.; Ebrey, T. G. *Biophys. J.* **1990**, *58*, 597.
(6) Tittor, J.; Oesterhelt, D. *FEBS Lett.* **1990**, *263*, 269.
(7) Dancshazy, Z.; Groma, G. I.; Oesterhelt, D.; Tittor, J. *FEBS Lett.* **1986**, *196*, 198.
(8) Varo, G.; Lanyi, J. K. *Biochemistry* **1991**, *30*, 5008.
(9) Oesterhelt, D. *Struct. Biol.* **1998**, *8*, 489.
(10) Luecke, H.; Schobert, B.; Richter, H.-T.; Cartailler, J.-P.; Lanyi, J. K. *Science* **1999**, *286*, 255.
(11) Korenstein, R.; Hess, B. *Nature* **1977**, *270*, 184.
(12) Varo, G.; Lanyi, J. K. *Biophys. J.* **1991**, *59*, 313.
(13) Dyukova, T. V.; Lukashev, E. P. *Thin Solid Films* **1996**, *283*, 1.
(14) Weik, M.; Zaccai, G.; Dencher, N. A.; Oesterhelt, D.; Hauss, T. *J. Mol. Biol.* **1998**, *275*, 625.
(15) Oesterhelt, D.; Hess, B. *Eur. J. Biochem.* **1973**, *37*, 316−326.
(16) Hampp, N.; Bräuchle, C.; Oesterhelt, D. *Biophys. J.* **1990**, *58*, 83.
(17) Oesterhelt, D.; Stoeckenius, W. *Methods Enzymol.* **1974**, *31*, 667.
(18) Hampp, N.; Seitz, A.; Juchem, T.; Oesterhelt, D. *Proc. SPIE* **1999**, *3623*, 243.
(19) Lewis, A.; Albeck, Y.; Lange, Z.; Benchowski, J.; Weizman, G. *Science* **1997**, *275*, 1462.
(20) Wherret, B. S. *Synth. Met.* **1996**, *76*, (1-3), 3.
(21) Thoma, R.; Dratz, M.; Hampp, N. *Opt. Eng.* **1995**, *34*, 1345.
(22) Birge, R. R. *Computer* **1992**, *25*, 56.
(23) Miller, A.; Oesterhelt, D. *Biochim. Biophys. Acta* **1990**, *1020*, 57.
(24) Yoshida, M.; Ohno, K.; Takeuchi, Y.; Kagawa, Y. *Biochem. Biophys. Res. Commun.* **1977**, *75*, 1111.
(25) Bitting, H. C. J.; Jang, D. J.; El-Sayed, M. A. *Photochem. Photobiol.* **1990**, *51*, 593.
(26) Eisfeld, W.; Pusch, C.; Diller, R.; Lohrmann, R.; Stockburger, M. *Biochemistry* **1993**, *32*, 7196.
(27) Hess, B.; Korenstein, R.; Kuschmitz, D. *FEBS−Symp.* **1978**, *58*, 187.
(28) Korenstein, R.; Hess, B. *Methods Enzymol.* **1982**, *88*, 193.
(29) Varo, G.; Needleman, R.; Lanyi, J. K. *Biophys. J.* **1996**, *70*, 461.
(30) Cao, Y.; Varo, G.; Chang, M.; Ni, B.; Needleman, R.; Lanyi, J. K. *Biochemistry* **1991**, *30*, 10972.
(31) Hatanaka, M.; Kandori, H.; Maeda, A. *Biophys. J.* **1997**, *73*, 1001.
(32) Ganea, C.; Gergely, C.; Ludmann, K.; Varo, G. *Biophys. J.* **1997**, *73*, 2718.
(33) Essen, L.-O.; Siegert, R.; Lehmann, W. D.; Oesterhelt, D. *Proc. Natl. Acad. Sci. U.S.A.* **1998**, *95*, 11673.
(34) Balashov, S. P.; Imasheva, E. S.; Govindjee, R.; Ebrey, T. G. *Biophys. J.* **1996**, *70*, 473.
(35) Balashov, S. P.; Lu, M.; Imasheva, E. S.; Govindjee, R.; Ebrey, T. G.; Othersen, B., III; Chen, Y.; Crouch, R. K.; Menick, D. R. *Biochem.* **1999**, *38*, 2026.
(36) Alshuth, T.; Stockburger, M. *Photochem. Photobiol.* **1986**, *43*, 55.
(37) Althaus, T.; Stockburger, M. *Biochemistry* **1998**, *37*, 2807.
(38) Lin, G. C.; Awad, E. S.; El-Sayed, M. A. *J. Phys. Chem.* **1991**, *95*, 10442.